ORIGINAL ARTICLE

An impaired healing model of osteochondral defect in papain-induced arthritis

Xiangbo Meng [a,e,f], Sibylle Grad [b], Chunyi Wen [d], Yuxiao Lai [a,e,f], Mauro Alini [b], Ling Qin [a,c,e], Xinluan Wang [a,c,e,f,*]

[a] Translational Medicine R&D Center, Institute of Biomedical and Health Engineering, Shenzhen Institutes of Advanced Technology, Chinese Academy of Sciences, Shenzhen, China
[b] AO Research Institute Davos, Clavadelerstrasse 8, Davos Platz, 7270, Switzerland
[c] Musculoskeletal Research Laboratory, Department of Orthopaedics & Traumatology, The Chinese University of Hong Kong, Hong Kong SAR, China
[d] Interdisciplinary Division of Biomedical Engineering, Faculty of Engineering, The Hong Kong Polytechnic University, Hung Hom, Kowloon, Hong Kong SAR, China
[e] CAS-HK Joint Lab of Biomaterials, Joint Laboratory of Chinese Academic of Science and Hong Kong for Biomaterials, Translational Medicine Research and Development Center, Shenzhen Institutes of Advanced Technology of Chinese Academy of Sciences and the Chinese University of Hong Kong, China
[f] Shenzhen Engineering Research Center for Medical Bioactive Materials, Shenzhen Institutes of Advanced Technology, Chinese Academy of Sciences, Shenzhen, China

ARTICLE INFO

ABSTRACT

Background: Osteochondral defects (OCD) are common in osteoarthritis (OA) and difficult to heal. Numerous tissue engineering approaches and novel biomaterials are developed to solve this challenging condition. Although most of the novel methods can successfully treat osteochondral defects in preclinical trials, their clinical application in OA patients is not satisfactory, due to a high spontaneous recovery rate of many preclinical animal models by ignoring the inflammatory environment. In this study, we developed a sustained osteochondral defect model in osteoarthritic rabbits and compared the cartilage and subchondral bone regeneration in normal and arthritic environments.

Methods: Rabbits were injected with papain (1.25%) in the right knee joints (OA group), and saline in the left knee joints (Non-OA group) at day 1 and day 3. One week later a cylindrical osteochondral defect of 3.2 mm in diameter and 3 mm depth was made in the femoral patellar groove. After 16 weeks, newly regenerated cartilage and bone inside the defect were evaluated by micro-CT, histomorphology and immunohistochemistry.

Results: One week after papain injection, extracellular matrix in the OA group demonstrated dramatically less safranin O staining intensity than in the non-OA group. Until 13 weeks of post-surgery, knee width remained significantly higher in the OA group than the non-OA control group. Sixteen weeks after surgery, the OA group had 11.3% lower International Cartilage Regeneration and Joint Preservation Society score and 32.5% lower O'Driscoll score than the non-OA group. There were less sulfated glycosaminoglycan and type II collagen but 74.1% more MMP-3 protein in the regenerated cartilage of the OA group compared with the non-OA group. As to the regenerated bone, bone volume fraction, trabecular thickness and trabecular number were all about 28% lower, while the bone mineral density was 26.7% higher in the OA group compared to the non-OA group. Dynamic histomorphometry parameters including percent labeled perimeter, mineral apposition rate and bone formation rate were lower in the OA group than in the non-OA group. Immunohistochemistry data showed that the OA group had 15.9% less type I collagen than the non-OA group.

Conclusion: The present study successfully established a non-self-healing osteochondral defect rabbit model in papain-induced OA, which was well simulating the clinical feature and pathology. In addition, we confirmed that both cartilage and subchondral bone regeneration were further impaired in arthritic environment.

The translational potential of this article: The present study provides an osteochondral defect in a small osteoarthritic model. This non-self-healing model and the evaluation protocol could be used to evaluate the efficacy and study the mechanism of newly developed biomaterials or tissue engineering methods preclinically; as methods tested in reliable preclinical models are expected to achieve improved success rate when tested clinically for treatment of OCD in OA patients.

Introduction

Osteoarthritis (OA) is one of the most prevalent joint diseases in the elderly [1], which leads to pain, stiffness and swelling of whole articular joint. The cartilage lesions caused by OA always extend deeply into subchondral bone and further develop into osteochondral defects (OCD) [2]. As cartilage lacks blood supply and innervation, its poor healing ability makes it difficult to repair [3]. In addition, the cartilage and subchondral bone possess different microstructure and physiological function. So, the treatment of OCD in OA patients (OA-OCD) remains a significant clinical challenge.

Tissue engineering (TE) approaches and biomaterials have emerged for the repair of cartilage defects and damages to the subchondral bone and have shown potential in restoring the joint's function [4]. In recent decades many biomaterials were evaluated in preclinical OCD animal models and achieved successful efficacy [5]. However, there was poor osteochondral repair in clinical trials. Many factors may contribute to the unsatisfying results, such as biological environment and biomechanical fixations of OC scaffolds to the host tissue. The inflammatory environment is another important factor, which has been ignored in most of the preclinical tests [6].

Inflammatory cytokines secreted by the inflammatory synovium contribute substantially to the pathogenesis of OA [7,8]. In patients with OA, levels of both IL-1β and TNF TNF-α are elevated in the synovial fluid, synovial membrane, subchondral bone and cartilage [7]. IL-1β and TNF-α downregulate the synthesis of major extracellular matrix (ECM) components by inhibiting anabolic activities of chondrocytes. IL-1β reduces type II collagen and aggrecan expression, and down-regulates proteoglycan synthesis through suppression of β-1, 3-glucuronyltransferase I [9]. Similarly, TNF-α has been shown to suppress the synthesis of proteoglycan, link protein and type II collagen in chondrocytes [10]. Proinflammatory cytokines such as IL-1β and TNF-α directly or indirectly act on bone metabolism through the RANKL/RANK/OPG system [11]. Thus, it is hypothesized that the inflammatory micro-environment may also affect both cartilage and bone regeneration. However, there are few studies to investigate the efficacy of TE biomaterials to repair osteochondral defects in OA-OCD animal model. A total of 331 literatures were found with keywords "osteoarthritis" and "osteochondral defect" or "cartilage defect" using PubMed database. Only one report used OCD in spontaneously induced equine OA to evaluate the potential of a multi-layer scaffold to enhance osteochondral regeneration [12]. Although large animals have the most similar clinical lesions to humans, these animal models are limited by higher management costs and slower disease progression [13]. To improve the success rate of novel TE approaches, an OA-OCD small animal model is necessary.

Papain is a proteolytic enzyme that causes OA by releasing chondroitin sulfate from a protein-polysaccharide complex of the articular cartilage matrix and producing inflammatory cytokines (TNF-α and IL-1β) [14]. Along with these inflammatory cytokines, MMP levels and free radical products increase [15]. All of these factors induced by intra-articular injection of papain lead to arthritis symptoms in rabbits, which mimic the conditions found in human OA [16]. In this study, an OA-OCD rabbit model was established by intra-articular injection of papain followed by the creation of a cylindrical osteochondral defect in the femoral patellar groove. Systemic evaluations at 16 weeks post-surgery were performed to examine newly formed cartilage and bone using micro-CT, histomorphology and immunohistochemistry.

Materials and methods

Animals

New Zealand white rabbits (body weight: 2.5 kg–3.4 kg) were purchased from Southern Medical University Laboratory Animal Center (Guangzhou, China) and maintained in the normal breeding room at Shenzhen-Peking University-Hong Kong University of Science & Technology (Shenzhen-PKU-HKUST) Medical Center. All the procedures for animal experiments were approved by the institutional animal care and use committee of the Shenzhen Institutes of Advanced Technology, Chinese Academy of Sciences (SIAT-IRB-170718-WXL-A0360).

Osteochondral defect model of rabbit knee osteoarthritis

Study 1-Pilot study Five male New Zealand white rabbits were created knee osteoarthritis model in the right knee via intra-articularly injected with 0.2 mL papain (25.0 mg/mL) three times (1, 3, 7 days), at the same time the same volume of 0.9% saline was injected as a control in the left knee (non-OA group). After ten days, the osteochondral defects (4.0 mm diameter) were created using a surgical drill on the medial femoral condyle to a depth of 3 mm on the knee. The samples were collected at 12 weeks post-surgery. The process was illustrated in Fig. 1A.

Study 2-Formal study On the tenth and seventh days before surgical operation, eight rabbits were intra-articularly injected with 0.2 mL papain (12.5 mg/mL) to build a knee osteoarthritis model in the right knee (OA group); at the same time the same volume of 0.9% saline was injected as a control in the left knee (non-OA group). Then, OCD were performed on both knees. The rabbits were anaesthetized by an injection of 3.0% (w/v) pentobarbital sodium (50 mg/kg) into the ear-vein. After careful cleaning of the surgical site, a medial parapatellar incision was made to expose the femoral trochlear groove. A 3.2 mm diameter full-thickness osteochondral defect was created using a surgical drill on the femur trochlear groove to a depth of 3 mm. During the drilling process, the defects were irrigated with saline solution to prevent the local overheating. Subsequently the incisions were sutured layer by layer using a degradable suture (4-0 silk suture, Jinhuan, Shanghai, China). After the operation, Penicillin (50000 IU/kg) and Gentamicin (5 mg/kg) was intramuscularly injected for 3 days to prevent bacterial infections. The experiment was carried out over 16 weeks. The process was illustrated in Fig. 2A. During this period, the width of the knee joint was recorded once a week. Double fluorochrome labelling was performed by intra-muscular injection of calcein green and xylenol orange disodium salt administered 10 and 3 days before sacrifice.

Micro-computed tomography (micro-CT) analysis

The animals were sacrificed to evaluate the tissue regeneration in OCD by micro-CT, at week 16 post-surgery. The samples were harvested and fixed in 4% (w/v) buffered paraformaldehyde for 3 days, then stored in 70% ethanol solution at 4 °C. The samples were scanned using a micro-CT 100 scanner (Scanco Medical, Switzerland) with X-ray beam energy of 70 kV, beam intensity of 114 μA, integration time of 300 ms and voxel size of 16.4 μm. To assess subchondral bone regeneration, the defect region was identified as region of interest (ROI), 3.2 mm wide × 3 mm deep. The threshold was set at 375 mg HA/cm^3 to distinguish mature bone from soft tissue. The X-ray attenuation of rabbit knee articular cartilage was calculated using an image processing method according to reported methods [17]. The ROIs were selected at the same size on the new cartilage area in the defect site to calculate the average X-ray attenuation coefficient. The X-ray attenuation in this study was reported in Hounsfield units. The host bone ROI (3.2-mm diameter and 3.0-mm depth) near the osteochondral defect was also used for quantitative analysis.

Histological evaluation

After the micro-CT analysis, the samples were divided into two parts, one part (n = 4) was decalcified in 10% (w/v) ethylenediamine-tetra acetic acid (EDTA), dehydrated by a series of ethanol, embedded in paraffin, and cut into pieces longitudinally with an approximate thickness of 5 μm using a paraffin microtome (Leica RM 2235, Germany). Sections were stained with hematoxylin and eosin (H&E) to examine repair tissue morphology, composition and alignment, cell infiltration

and extracellular matrix production, toluidine blue (T-B) to assess the presence of proteoglycans, safranin-O/Fast green (S–F) to assess sGAG. The optical density of sGAG was semi-quantitatively calculated using Image-pro plus 6.0.

The histological sections were independently scored by three evaluators using a modified O'Driscoll histologic scoring [18], and scores were averaged. Cartilage repair in the OCD region was quantitatively evaluated with the International Cartilage Regeneration and Joint Preservation Society (ICRS) scoring system [19]. ICRS scoring system was used to rate cartilage repair tissue as grade IV (severe abnormality, 0–3 points), grade III (abnormal, 4–7 points), grade II (near normal, 8–11 points) or grade I (normal, 12 points) with respect to defect repair, degree of integration and macroscopic appearance.

For undecalcified bone, specimens (n = 4) were embedded in methyl methacrylate (MMA) and cut at 8 μm thickness using a tungsten steel knife (Leica 26166, Germany). Undecalcified sections were observed by fluorescence microscopy (Leica Dmi8, Germany) to determine the mineral apposition rate (MAR), percent labeled perimeter (%L.Pm) and bone formation rate (BFR/BS) of new bone formation by monitoring the distance and perimeter between the two labels.

Immunohistochemistry

Immunohistochemistry was performed to assess the extracellular matrix of newly formed bone and cartilage as described previously [20]. The following primary antibodies were used in this study; monoclonal mouse anti-type I collagen antibody (Novus Biologicals, US, 1 in 100 dilution), monoclonal mouse anti-type II collagen antibody (Novus Biologicals, US, 1 in 50 dilution), and mouse monoclonal anti-MMP-3 antibody (Proteintech, US, 1 in 100 dilution). Horseradish
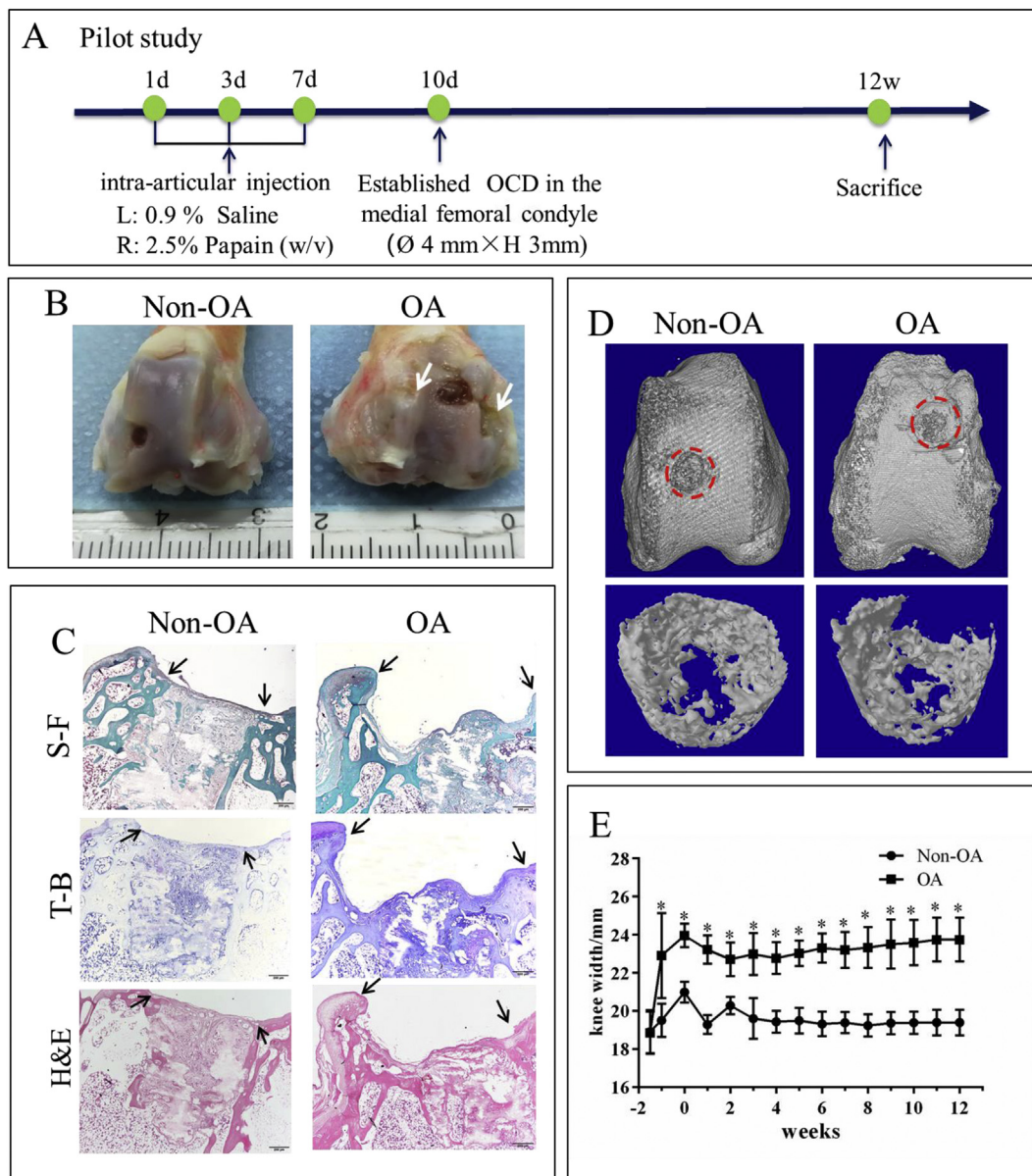

Fig. 1. Papain-induced OA caused severe cartilage damage in the pilot study. A: Diagram for establishing an OCD model in papain-induced OA rabbits in the pilot study. B: Macroscopic observation revealed that the cartilage surface in the OA group was severely damaged by papain 12 weeks after surgery, white arrow: rough surface indicating damaged cartilage. C: Histological analysis (S–F: safranin O-fast green, T–B: toluidine blue and H&E: hematoxylin and eosin) revealed that the cartilage self-repair was limited in both papain-induced OA and non-OA rabbits, black arrows: the margins of the defect. D: Micro-CT analysis showed less subchondral bone formation in the defect region. E: the change of knee width over time showed chronic swollen knee existed in the OA group. Data are shown as mean ± SEM, N = 5. Two-way ANOVA followed by Holm-Sidak's multiple comparison test were used to evaluate differences between OA and non-OA groups at the same time point. *$p < 0.05$.

peroxidase-conjugated secondary anti-rabbit and mouse immunoglobulin were used as appropriate, and the color reaction developed with 0.1% 3, 3-diaminobenzidine tetrachloride (DAB)/0.01% hydrogen peroxide. The integrated optical densities (IOD) of COL I, COL II and MMP-3 were semi-quantitatively calculated using Image-pro plus 6.0.

Statistics

Data were presented as mean ± SD. Statistical analysis was performed using GraphPad Prism 6.0 (GraphPad Software Inc., San Diego, CA, USA). Paired *t*-test or two-way ANOVA (data with different time points) followed by Holm-Sidak's multiple comparison test were used to evaluate differences between OA and non-OA groups. The differences were considered significant when $p < 0.05$.

Results

Optimization of the protocol based on pilot study

In a pilot study, the samples were harvested at week 12 post-operation. Compared with non-OA, articular cartilage surface was severely damaged in the OA group by injection of papain (Fig. 1B). Limited cartilage self-repair was found in both papain-induced OA and non-OA rabbits (Fig. 1C). Although more bone formation was found in the non-OA group, obvious cysts existed in both groups (Fig. 1D). Although knee width in the OA group kept higher level until 12 weeks indicating the presence of chronic inflammation (Fig. 1E), cartilage and bone regeneration was too poor to be used as an early OA-OCD model for evaluating the efficacy of TE biomaterials. Thus, we modified the protocol for the following study.

Damaged cartilage and inflammation in papain-induced OA group

On the tenth day after the first injection of papain, histological analysis showed that the cartilage in the OA group had less safranin O staining intensity in the extracellular matrix compared with the non-OA group (Fig. 2B). At week 16 post-operation, the defects were filled with newly formed tissues in both non-OA group and the OA group. The newly formed tissue was less transparent, and there was a clear boundary between the new tissue and the native cartilage, indicating that the self-repair was incomplete. Additionally, compared with non-OA, articular cartilage surface outside the defect was much rougher in the OA group
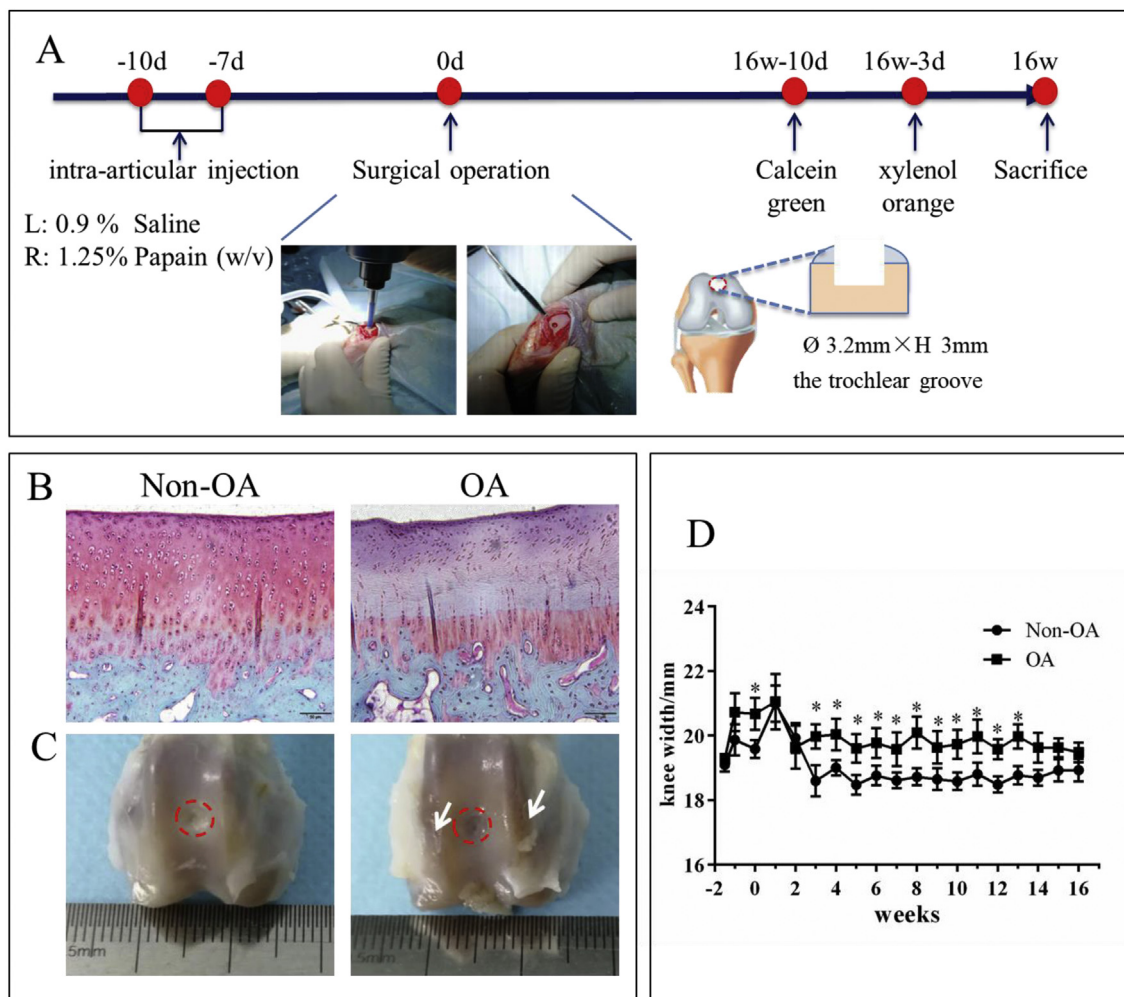

Fig. 2. Cartilage damage and chronic swollen knee in OA rabbits. A: Diagram for establishing an OCD model in papain-induced OA rabbits. On the tenth and seventh days before surgical operation, papain or saline was articularly injected into the right or left knee, respectively. Then, OCD (3.2 mm diameter × 3.0 mm depth) was made in the femoral trochlear center. Knee width was recorded every week. Double fluorochrome labelling was performed by intra-muscular injection of calcein and xylenol orange disodium salt administered 10 and 3 days before sacrifice. 16 weeks after surgery, samples were harvested for analysis. B: Safranin O-fast green staining showed cartilage erosion and loss of proteoglycan in the OA group on the tenth day after the first injection of papain; C: macroscopic observation of the knee at 16 weeks after surgery, white arrow: rough surface indicating damaged cartilage; D: the change of knee width over time showed chronic swollen knee existed in the OA group. Data are shown as mean ± SEM, N = 8. Two-way ANOVA followed by Holm-Sidak's multiple comparison test were used to evaluate differences between OA and non-OA groups at the same time point. *$p < 0.05$.

indicating more severe cartilage degradation (Fig. 2C). In addition, on the tenth day after injection of papain or saline, knee width in the OA group was significantly higher than that in the non-OA group. Surgery increased knee width on both groups at one-week post-operation. However, knee width in the non-OA group decreased to normal afterwards, while that in the OA group kept a higher level until 13 weeks, which suggests the presence of chronic inflammation in the OA knee (Fig. 2D).

Histological evaluation of the cartilage regeneration

As shown in Fig. 3A, H&E staining revealed that the articular cartilage of the non-OA group was smooth and intact. In contrast, the joint cartilage of the OA group showed noticeable degradation, including irregular superficial zone, degenerative matrix and disarranged chondrocytes. The new cartilage of the non-OA group exhibited an intense staining of both safranin O-fast green (S-F) and toluidine blue (T-B) and was able to integrate with the adjacent cartilage. At high magnification, the chondrocyte arrangement in the new cartilage displayed a similar pattern to that of hyaline cartilage. In contrast, new tissues within the OA group showed limited bone and cartilage repair with poor quality for up to 16 weeks. Cysts and limited regeneration of subchondral bone were present in both groups.

ICRS score of the non-OA group (7.7 ± 2.5) was 11.3% higher than the OA group (6.9 ± 1.2) ($P < 0.05$) (Fig. 3B). Based upon the modified O'Driscoll scoring system, the repair score of the non-OA group (16.0 ± 3.5) was 32.5% higher than the OA group (10.8 ± 1.3) ($P < 0.05$)

(Fig. 3C). The average sGAG optical density of the non-OA group (259.9 ± 58.1) was 62.6% higher than that of the OA group (97.0 ± 42.5) ($P < 0.05$) (Fig. 3D).

Micro-CT quantification of newly formed bone and adjacent host bone

Micro-CT was used to evaluate the host bone adjacent to the defect site and newly formed bone in the defect site in both the non-OA and OA groups at week 16 after surgery. The self-repair of the subchondral bone in both the OA group and the non-OA group was limited, as there was a large cavity in the defect region (Fig. 4A). Quantitative results showed that as to the host bone, OA group had 27.7% higher bone mineral density (BMD) than the non-OA group ($P < 0.01$) (Fig. 4B), but the bone volume fraction (BV/TV) was similar in both groups ($P > 0.05$) (Fig. 4C).

As to newly formed bone in the defect area, morphometric data of the defect areas of OA and non-OA group were also compared. The ratio of BV to TV decreased substantially from 25.23% in the non-OA group to 19.05% in the OA group ($P < 0.05$). Compared with the non-OA group, the trabecular thickness (Tb.Th) was decreased from 0.27 μm to 0.20 μm in the OA group at 16 weeks post-surgery ($P < 0.05$). The trabecular number with lower value indicating disruption of microarchitecture of the defect area, was decreased from 1.39 μm^{-1} to 1.10 μm^{-1} ($P < 0.05$). The trabecular separation (Tb.Sp) and BMD of the OA group increased significantly (by 20.7% and 26.7% respectively) compared to the non-OA group ($P < 0.05$ for both) (Fig. 4D-H). The X-ray attenuation value of the OA group was 27.1% higher when compared with that in the non-OA
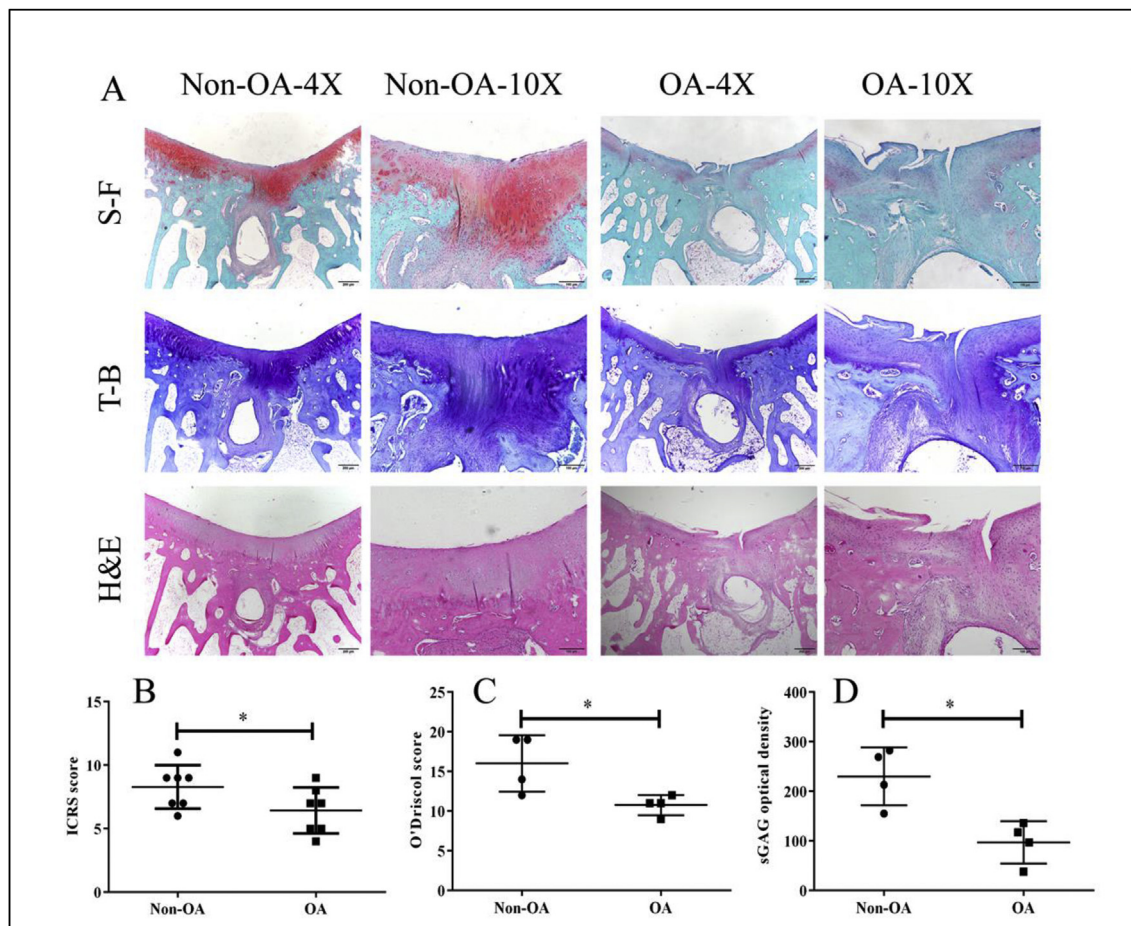

Fig. 3. Histological analysis of cartilage repair at 16 weeks post-surgery. A: Representative histological images of newly formed tissue in OCD region at week 16 post-surgery. Safranin O-fast green (S–F), toluidine blue (T–B) and hematoxylin and eosin (H&E) staining in the non-OA group showed enhanced cartilage and subchondral bone repair, compared to the OA group. There is a large subchondral cyst in the non-OA group and OA group. The arrows denote the margins of the defect. B: International Cartilage Repair Regeneration and Joint Preservation Society (ICRS) scoring; C: The modified O'Driscoll histological scoring; D: The sGAG optical density. Data are shown as mean ± SD, N = 4, Paired *t*-test were used to evaluate differences between OA and non-OA groups. *$p < 0.05$.
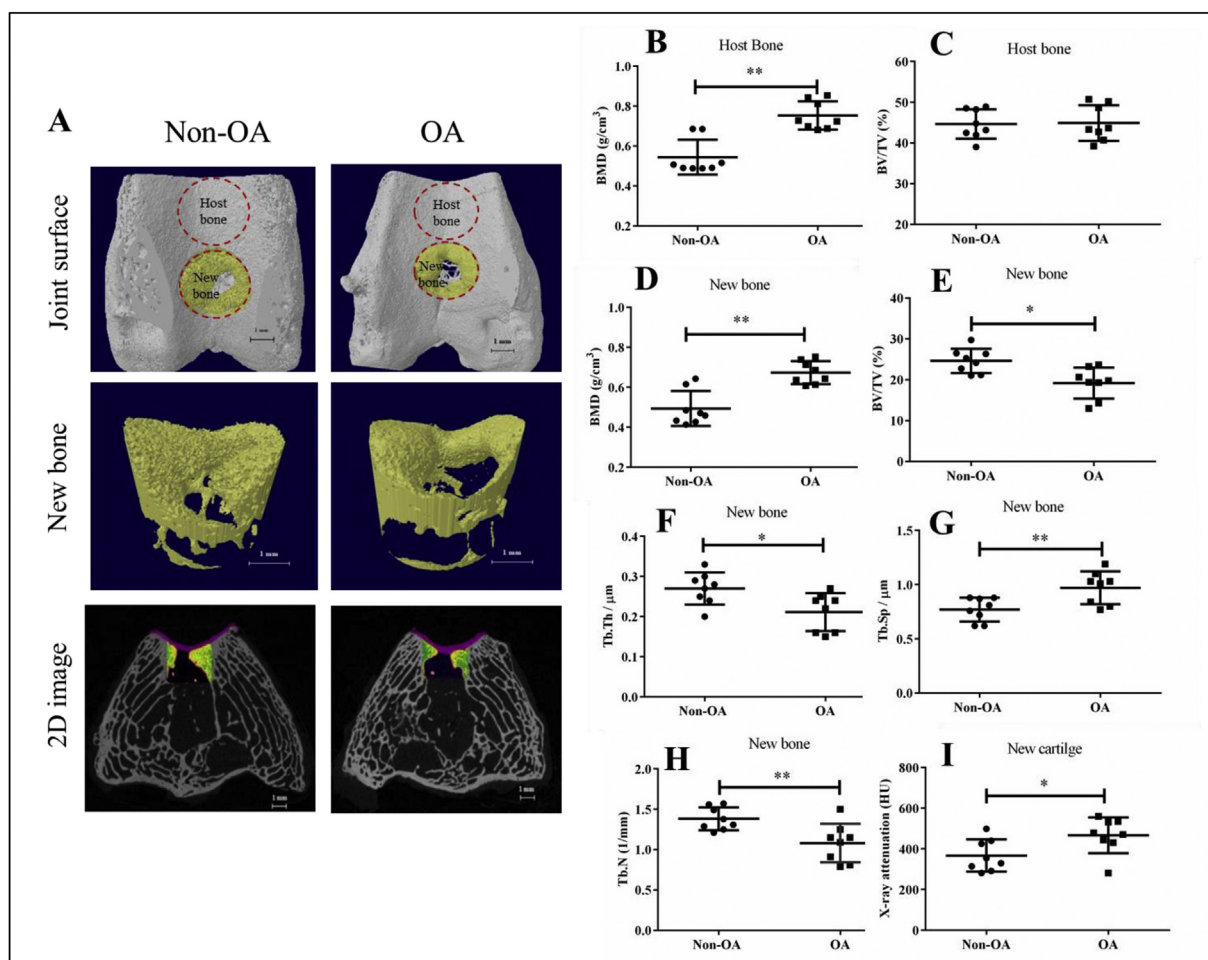
Fig. 4. Micro-CT analysis showed that the subchondral bone and cartilage formation in the defect area of the OA group was less than that of the non-OA group. A: The reconstructed images showed the joint surfaces, the newly formed bone in OCD region (new bone) and 2D image of the distal femur OCD site (red: cartilage). B–C: The quantitative micro-CT data of bone mineral density (BMD), bone volume fraction (BV/TV) of the host bone. D–H: The quantitative micro-CT data of bone mineral density (BMD), bone volume fraction (BV/TV), trabecular thickness (Tb.Th), trabecular separation (Tb.Sp) and trabecular number (Tb.N) of newly formed bone. I: The X-ray attenuation value of the newly formed cartilage in OCD region. Data are shown as mean ± SD, N = 8. Paired t-test were used to evaluate differences between OA and non-OA groups. $^*p < 0.05$, $^{**}p < 0.01$.

group (from 367.1 ± 78.9 HU to 466.0 ± 87.1 HU, $P < 0.05$) (Fig. 4I).

Assessment of dynamic parameters

Double fluorochrome labelling was performed by intramuscular injection of calcein and xylenol orange disodium salt administered 10 and 3 days before sacrifice. The newly formed bone showed abundant labeled surfaces compared to the host area at week 16 post-surgery (Fig. 5A). Magnified images clearly showed double labeled-lines (green and red) in both groups (Fig. 5B–C). Percent labeled perimeter (%L.Pm), mineral apposition rate (MAR) and bone formation rate (BFR/BS) of the OA group were 28.6%, 15.7% and 49.3% lower than those of the non-OA group, respectively (Fig. 5D–F).

Immunohistochemical staining for both cartilage and bone specific proteins

Immunohistochemical (IHC) staining of COL I and COL II was performed to assess the extracellular matrix of newly formed bone and cartilage. The brown areas indicate positive expression of COL I and COL II in regenerated tissues. The visualization of osteogenic marker collagen I (COL I) and chondrogenic marker collagen II (COL II) is shown in Fig. 6A. COL I staining and COL II staining were located in newly formed bone and cartilage as detected histologically, respectively. After 16 weeks, the semi-quantitative results showed that the IOD of COL I and

COL II in the non-OA group were 15.9% and 13.4% higher than those in the OA group ($P < 0.05$) (Fig. 6B). In addition, the expression of MMP-3 protein in the OA group was 74.1% higher than in the non-OA group ($P < 0.05$), and the MMP-3 protein was mainly located in the superficial zone of the cartilage.

Discussion

Osteochondral defects are common in osteoarthritis and challenging to heal. Numerous tissue engineering biomaterials have been developed and most of them were evaluated in normal OCD pre-clinical animal models, ignoring the inflammatory environment. In this study we describe an osteochondral defect in papain-induced osteoarthritis rabbit model and confirm that arthritis further impairs cartilage and bone healing. We used micro-CT, conventional histology, immunohistochemistry and histomorphometry to systematically investigate cartilage and subchondral bone regeneration in OA-OCD rabbits. The results demonstrated that both cartilage and subchondral bone regeneration were further impaired in arthritic environment, and the data were summarized in Table 1.

Papain successfully induced typical symptoms of early OA

It has been reported that papain injection increased the expression of
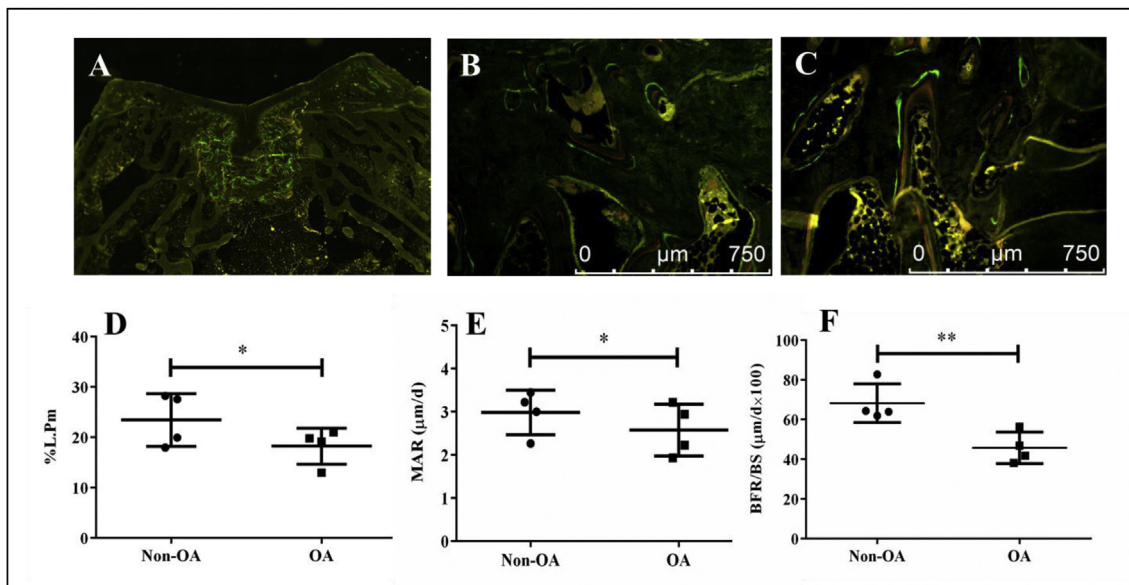
Fig. 5. Dynamic histomorphometry of newly formed tissue in OCD region. A–C: Representative fluorescence images of subchondral bone in OCD region (A: Gross fluorescence image, B: Non-OA group, C: OA group). D–F: Quantification of percent labeling perimeter (%L.Pm), mineral apposition rate (MAR) and bone formation rate (BFR/BS). Data are shown as mean $\pm$ SD, N = 4. Paired *t*-test were used to evaluate differences between OA and non-OA groups. *$p < 0.05$ and **$p < 0.01$.

IL-1β and TNF-α in serum and synovial fluid [21,22], which caused an inflammatory micro-environment. Our experimental model of OA induction by papain injection was effective in triggering an arthritic response as evidenced by increased joint width, cartilage degradation in terms of the reduction of safranin O staining intensity, and subchondral sclerosis (i.e. higher BMD of host subchondral bone). These outcomes were consistent with the previous findings and typical symptoms of early OA [23]. It was reported that the superficial cells of synovial tissue
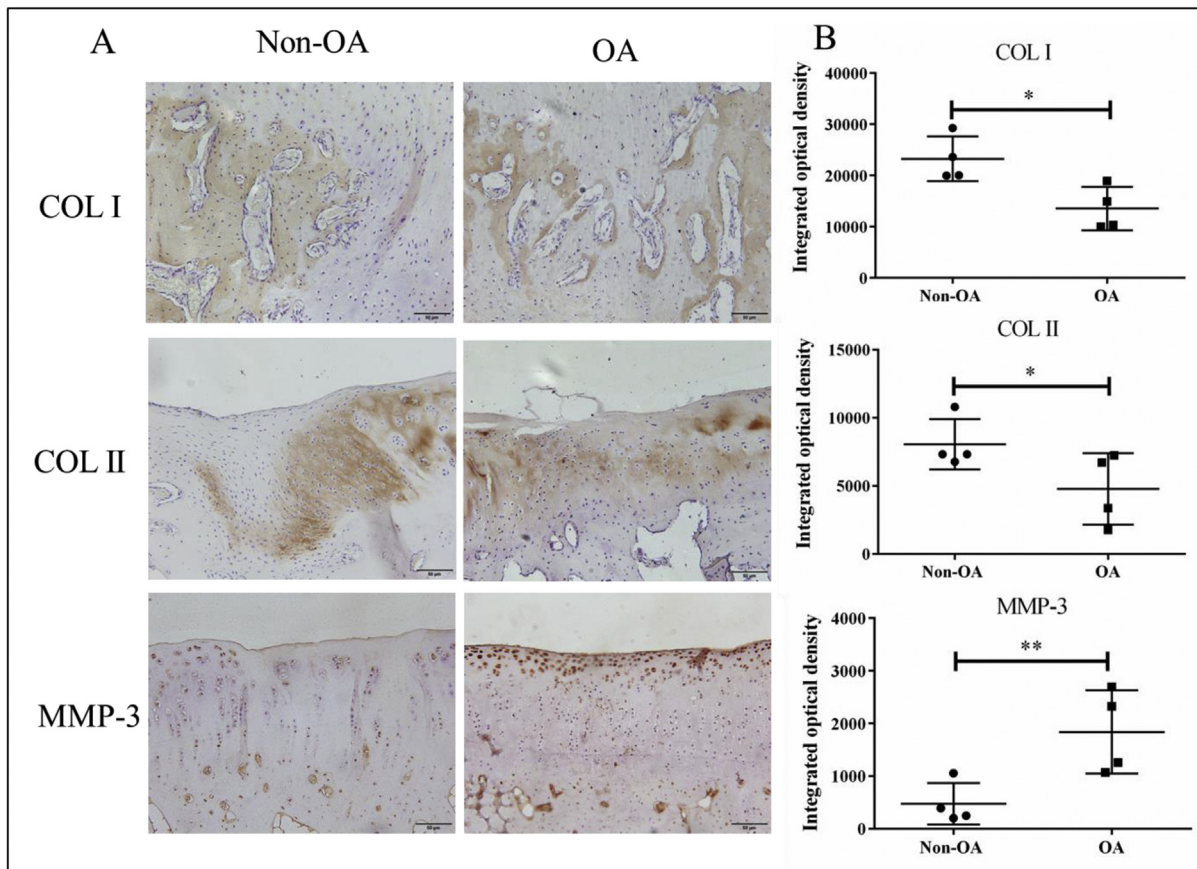

Fig. 6. Immunohistochemical (IHC) staining of collagen type I (COL I), collagen type II (COL II) and MMP-3 in newly formed tissue in OCD region. A: Representative images of IHC of COL I, COL II and MMP-3. B: The semi-quantitative results of COL I, COL II and MMP-3. Data are shown as mean $\pm$ SD, N = 4. Paired *t*-test were used to evaluate differences between OA and non-OA groups. *$p < 0.05$ and **$p < 0.01$.

Table 1

Summarized table with quantitative parameters (mean $\pm$ SD) in Non-OA and OA groups. Paired *t*-test were used to evaluate differences between OA and non-OA groups.

Parameters	unit	Non-OA group	OA group	*p* value
ICRS score	/	7.71 ± 2.52	6.93 ± 1.20	0.0107
modified O'Driscoll histological score	/	16.01 ± 3.51	10.83 ± 1.30	0.0214
sGAG optical density	/	259.93 ± 58.10	96.96 ± 42.93	0.0258
BMD-host bone	g/cm³	0.54 ± 0.07	0.75 ± 0.06	0.0006
BMD-new bone	g/cm³	0.49 ± 0.07	0.67 ± 0.05	0.0004
BV/TV-host bone	%	44.66 ± 3.19	44.92 ± 3.84	0.8793
BV/TV-new bone	%	24.63 ± 2.61	19.19 ± 3.35	0.0106
X-ray attenuation	HU	367.11 ± 78.90	466.45 ± 87.12	0.0485
Tb.Th	μm	0.27 ± 0.04	0.21 ± 0.04	0.0110
Tb.N	1/mm	1.38 ± 0.12	1.08 ± 0.21	0.0096
Tb.Sp	μm	0.77 ± 0.096	0.97 ± 0.133	0.0096
%L.Pm	%	23.40 ± 4.06	18.23 ± 2.78	0.0325
MAR	μm/d	2.98 ± 0.39	2.57 ± 0.47	0.0436
BFR/BS	μm/d*100	68.27 ± 7.54	45.76 ± 6.08	0.0011
IOD of COL I	/	23,237.52 ± 3381.26	13,542.56 ± 3289.49	0.0386
IOD of COL II	/	8048.04 ± 1429.65	4771.63 ± 2039.97	0.0329
IOD of MMP-3	/	476.98 ± 306.49	1839.62 ± 613.62	0.0064

thickened, and a small number of inflammatory cells infiltrated in the early stage of papain-induced OA [24], which induced synovial inflammation with accumulation of cartilage and bone debris in the inferior capsule and later capsular thickening [25]. However, in this study we only focused on the cartilage and subchondral bone in the joint, ignoring the synovial tissue and capsule. Thus, one limitation of our study is that we did not test the pro-inflammatory response in the synovial fluid as well as the synovial tissue.

In an animal model aimed to evaluate the efficacy of biomaterials, limited self-repair is necessary but it should keep a proper range [26]. If the damage is too severe to be repaired, the difference among various biomaterials can not identified, so we optimized the protocol by reducing the concentration of papain from 25.0 mg/mL to 12.5 mg/mL to reduce the inflammation, decreasing the diameter of OCD from 4 to 3.5 mm for better cartilage regeneration, and prolonging the duration from 12 to 16 weeks for more newly formed bone. However, bone formation at 16 weeks after surgery was still ongoing, which implies that longer observation may be needed for subchondral bone regeneration in the future study. In addition, the OCD site was changed from the medial femoral condyle to femoral trochlear center, because it is difficult to make identical in each rabbit at the medial femoral condyle practically, although it is more closely to human OA.

Impaired cartilage regeneration in OA group

Damaged articular cartilage has poor self-repair capacity [27]. The self-repair depends on the size, depth and location of the defect [4]. In our study, limited self cartilage repair was found in both papain-induced OA and non-OA rabbits. It was reported that papain injection destroyed most of the chondrocyts and instead, mesenchymal cells in the transition zone were found actively engaged in the repair of articular cartilage [28]. Further, IL-1β down-regulated xylosyltransferase-I (XT-I) gene expression, led to decreased glycosaminoglycans (GAG) biosynthesis onto proteoglycan (PG) molecules [29]. In addition, inflammatory cytokines induced miR-29b expression in BMSC which inhibited collagen I and III expression, thus resulting in formation of inferior fibrocartilage instead of hyaline cartilage. Furthermore, higher miR-29b expression promoted apoptosis, thereby either preventing excessive cell growth or reducing the number of BMSC undergoing chondrogenesis [30]. This study showed consistant results with respect to lower ICRS score and modified

O'Driscoll score, less COL II and higher MMP-3 in the newly regenerated cartilage in the OA group compared to the non-OA group. In addition, papain injection influenced the composition of the newly formed extracellular matrix (ECM) of cartilage in terms of PG and collagen. It implys that we should pay more attention to modifying the inflammatory and catabolic environment for cartilage repair in OA patients.

Impaired subchondral bone regeneration in OA group

In our study, papain injection induced subchondral sclerosis in term of higher BMD in the host bone of the OA group than the non-OA group. This phenomenon was also reported in previous animal studies [25]. BV/TV did not differ between early OA and non-OA, which is quite similar with the clinical data [31]. Interestingly, the newly formed bone in the OA group had less bone volume percent (BV/TV) but higher BMD. To our knowledge, it is the first time to demonstrate newly formed sclerotic subchondral bone in OA. Previously, it was reported that overloaded OA subchondral bone osteoblasts expressed a pro-angiogenic and pro-inflammatory phenotype which contributes to explain the structural changes (sclerosis) in OA subchondral bone [32]. However, in our model, femoral trochlea is a non-loading area, so the mechanical factor might not play an important role in this model. Another explanation was that osteoblasts derived from OA sclerotic bone produce less type I collagen with aberrant Col1 α1/α2 ratio and poor mineralization capability [33]. The mineralization status of regenerated tissue was demonstrated by dynamic histomorphometry data. Mineralizing surface (%L.Pm) displays new mineralized bone was being deposited during the period of fluorescence labeling. Mineral apposition rate (MAR) is the measurement of the linear rate of new bone deposition. Bone formation rate is calculated by multiplying the mineralizing surface by the mineral apposition rate [34]. We found that mineralizing surface (%L.Pm), mineral apposition rate (MAR) and bone formation rate (BFR/BS) were all significantly lower in the OA group compared to the non-OA group, which indicated poor mineralization capability and lower BV/TV in OA. Microscopic images demonstrated that Grade IV OA bone showed higher crystallinity of the mineral content, increased modulus and hardness compared with grade I OA bone [35]. In addition, the intra-cellular environment of sclerotic subchondral bone might be more acidotic and hypoxic compared with the non-sclerotic subchondral bone [36].

Limitations of this study

It was reported that there was no significant influence of gender on the presence of osteoarthritis [37]. Although most have used male rabbits for investigating the repair of osteochondral defect, some studies have used randomly selected male and female rabbits [38], and some used only female animals [39]. However, up to now there have been no reports investigating the gender difference about self-healing ability in osteochondral defects. It needs to be further clarified in the future.

Due to a lower intraindividual variability, compared to unilateral operation, bilateral design significantly reduced the sample size requirements for articular cartilage tissue engineering. However, particularly differences in the mechanical loading of the defects caused significantly different osteochondral repair between bilateral and unilateral defects [40]. Thus, the results obtained from the limbs of bilaterally operated animals cannot be compared conclusively with the limbs of unilaterally operated animals. In addition, due to its simultaneous affection of both limbs, the bilateral study design is of limited suitability whenever postoperative unloading of the treated joint is necessary or when gait analyses are to be performed [40].

Conclusion

In summary, the present study successfully built a non-self-healing osteochondral defect rabbit model in papain-induced OA, which was well simulating the clinical feature and pathology. We confirmed that

both cartilage and subchondral bone regeneration were further impaired in arthritic environment. This successfully established OA-OCD model and the evaluation protocol could be used to evaluate the efficacy and study the mechanism of newly developed biomaterials or tissue engineering methods preclinically, which might improve success rate of novel TE biomaterials when used in clinal trial for treatment of OCD in OA patients.

Authorship

X.L. Wang: Conception and design of study, Drafting the manuscript.

X.B. Meng: Conception and design of study, acquisition of data, Drafting the manuscript.

L. Qin: Conception and design of study, revising the manuscript critically for important intellectual content.

S. Grad: Drafting the manuscript.

C.Y. Wen: Revising the manuscript critically for important intellectual content.

Y.X. Lai: Revising the manuscript critically for important intellectual content.

M. Alini: Revising the manuscript critically for important intellectual content.

Approval of the version of the manuscript to be published (the names of all authors must be listed): X.B. Meng, S. Grad, C.Y. Wen, Y.X. Lai, M. Alini, L. Qin, X.L. Wang.

Conflict of Interest

The authors have no conflicts of interest to disclose in relation to this article.

References

[1] Iijima H, Shimoura K, Aoyama T, Takahashi M. Biomechanical characteristics of stair ambulation in patients with knee OA: a systematic review with meta-analysis toward a better definition of clinical hallmarks. Gait Posture 2018;62:191–201.

[2] Re'em T, Witte F, Willbold E, Ruvinov E, Cohen S. Simultaneous regeneration of articular cartilage and subchondral bone induced by spatially presented TGF-beta and BMP-4 in a bilayer affinity binding system. Acta Biomater 2012;8(9):3283–93.

[3] Guo W, Zheng X, Zhang W, Chen M, Wang Z, Hao C, et al. Mesenchymal stem cells in oriented PLGA/ACECM composite scaffolds enhance structure-specific regeneration of hyaline cartilage in a rabbit model. Stem Cell Int 2018;2018: 6542198.

[4] Deng C, Chang J, Wu C. Bioactive scaffolds for osteochondral regeneration. J Orthop Translat 2019;17:15–25.

[5] Meng X, Ziadlou R, Grad S, Alini M, Wen C, Lai Y, et al. Animal models of osteochondral defect for testing biomaterials. Biochem Res Int 2020;2020:9659412.

[6] Zhang Y, Pizzute T, Pei M. Anti-inflammatory strategies in cartilage repair. Tissue Eng B Rev 2014;20(6):655–68.

[7] Kapoor M, Martel-Pelletier J, Lajeunesse D, Pelletier JP, Fahmi H. Role of proinflammatory cytokines in the pathophysiology of osteoarthritis. Nat Rev Rheumatol 2011;7(1):33–42.

[8] Gallo J, Raska M, Kriegova E, Goodman SB. Inflammation and its resolution and the musculoskeletal system. J Orthop Translat 2017;10:52–67.

[9] Stove J, Huch K, Gunther KP, Scharf HP. Interleukin-1beta induces different gene expression of stromelysin, aggrecan and tumor-necrosis-factor-stimulated gene 6 in human osteoarthritic chondrocytes in vitro. Pathobiology 2000;68(3): 144–9.

[10] Seguin CA, Bernier SM. TNFalpha suppresses link protein and type II collagen expression in chondrocytes: role of MEK1/2 and NF-kappaB signaling pathways. J Cell Physiol 2003;197(3):356–69.

[11] Walsh MC, Choi Y. Biology of the RANKL-RANK-OPG system in immunity, bone, and beyond. Front Immunol 2014;5:511.

[12] Stack JD, Levingstone TJ, Lalor W, Sanders R, Kearney C, O'Brien FJ, et al. Repair of large osteochondritis dissecans lesions using a novel multilayered tissue engineered construct in an equine athlete. J Tissue Eng Regen M 2017;11(10):2785–95.

[13] Teeple E, Jay GD, Elsaid KA, Fleming BC. Animal models of osteoarthritis: challenges of model selection and analysis. AAPS J 2013;15(2):438–46.

[14] Lampropoulou-Adamidou K, Lelovas P, Karadimas EV, Liakou C, Triantafillopoulos IK, Dontas I, et al. Useful animal models for the research of osteoarthritis. Eur J Orthop Surg Traumatol 2014;24(3):263–71.

[15] Johanne MP, Nada A, Pelletier JP. Cytokines and their role in the pathophysiology of osteoarthritis. Front Biosci 1999;4(1–3):694–703.

[16] Patel DV, Sawant MG, Kaur G. Evaluation of anti-osteoarthritic activity of Vigna mungo in papain induced osteoarthritis model. Indian J Pharmacol 2015;47(1): 59–64.

[17] Li XF, Cai XR, Fan F, Niu HJ, Li SY, Li DY, et al. Observation of sGAG content of human hip joint cartilage in different old age groups based on EPIC micro-CT. Connect Tissue Res 2015;56(2):99–105.

[18] Frenkel SR, Bradica G, Brekke JH, Goldman SM, Ieska K, Issack P, et al. Regeneration of articular cartilage–evaluation of osteochondral defect repair in the rabbit using multiphasic implants. Osteoarthritis Cartilage 2005;13(9): 798–807.

[19] van den Borne MP, Raijmakers NJ, Vanlauwe J, Victor J, de Jong SN, Bellemans J, et al. International Cartilage Repair Society (ICRS) and oswestry macroscopic cartilage evaluation scores validated for use in Autologous Chondrocyte Implantation (ACI) and microfracture. Osteoarthritis Cartilage 2007;15(12): 1397–402.

[20] Henson FM, Davies ME, Jeffcott LB. Equine dyschondroplasia (osteochondrosis)–histological findings and type VI collagen localization. Vet J 1997;154(1):53–62.

[21] Hu XB, Kang RR, Tang TT, Li YJ, Wu JY, Wang JM, et al. Topical delivery of 3,5,4-trimethoxy-trans-stilbene-loaded microemulsion-based hydrogel for the treatment of osteoarthritis in a rabbit model. Drug Deliv Transl Re 2019;9(1):357–65.

[22] Cheng F, Yan FF, Liu YP, Cong Y, Sun KF, He XM. Dexmedetomidine inhibits the NF-kappaB pathway and NLRP3 inflammasome to attenuate papain-induced osteoarthritis in rats. Pharm Biol 2019;57(1):649–59.

[23] Tomazoni SS, Leal-Junior EC, Pallotta RC, Teixeira S, de Almeida P, Lopes-Martins RA. Effects of photobiomodulation therapy, pharmacological therapy, and physical exercise as single and/or combined treatment on the inflammatory response induced by experimental osteoarthritis. Laser Med Sci 2017;32(1):101–8.

[24] Han GY, Ling PX, Wang FS, Wang GL, Shao HR. Comparison study on knee osteoarthritis in rabbits induced by different concentrations of papain. Zhong Guo Gu Shang 2012;25(5):424–9.

[25] Bentley G. Papain-induced degenerative arthritis of the hip in rabbits. J Bone Joint Surg Br 1971;53(2):324–37.

[26] Li Y, Chen SK, Li L, Qin L, Wang XL, Lai YX. Bone defect animal models for testing efficacy of bone substitute biomaterials. J Orthop Translat 2015;3:95–104.

[27] Lee WY, Wang B. Cartilage repair by mesenchymal stem cells: clinical trial update and perspectives. J Orthop Translat 2017;9:76–88.

[28] Moriizumi T, Yamashita N, Okada Y. Papain-induced changes in the Guinea pig knee joint with special reference to cartilage healing. Virchows Arch B 1986;51(6): 461–74. Cell Pathol Incl Mol Pathol.

[29] Venkatesan N, Barre L, Bourhim M, Magdalou J, Mainard D, Netter P, et al. Xylosyltransferase-I regulates glycosaminoglycan synthesis during the pathogenic process of human osteoarthritis. PloS One 2012;7(3):e34020.

[30] Mayer U, Bendit A, Grassel S. miR-29b regulates expression of collagens I and III in chondrogenically differentiating BMSC in an osteoarthritic environment. Sci Rep 2017;7(1):13297.

[31] Klose-Jensen R, Hartlev LB, Boel LWT, Laursen MB, Stengaard-Pedersen K, Keller KK, et al. Subchondral bone turnover, but not bone volume, is increased in early stage osteoarthritic lesions in the human hip joint. Osteoarthritis Cartilage 2015;23(12):2167–73.

[32] Henrotin Y, Pesesse L, Sanchez C. Subchondral bone and osteoarthritis: biological and cellular aspects. Osteoporos Int 2012;23(Suppl 8):S847–51.

[33] Weber A, Chan PMB, Wen C. Do immune cells lead the way in subchondral bone disturbance in osteoarthritis? Prog Biophys Mol Biol 2017;148:21–31.

[34] Kulak CA, Dempster DW. Bone histomorphometry: a concise review for endocrinologists and clinicians. Arq Bras Endocrinol Metabol 2010;54(2):87–98.

[35] Zuo Q, Lu S, Du Z, Friis T, Yao J, Crawford R, et al. Characterization of nano-structural and nano-mechanical properties of osteoarthritic subchondral bone. BMC Muscoskel Disord 2016;17(1):367.

[36] Yang G, Zhang H, Chen T, Zhu W, Ding S, Xu K, et al. Metabolic analysis of osteoarthritis subchondral bone based on UPLC/Q-TOF-MS. Anal Bioanal Chem 2016;408(16):4275–86.

[37] Arzi B, Wisner ER, Huey DJ, Kass PH, Hu J, Athanasiou KA. A proposed model of naturally occurring osteoarthritis in the domestic rabbit. Lab Anim 2011;41(1): 20–5.

[38] Wang ZJ, An RZ, Zhao JY, Zhang Q, Yang J, Wang JB, et al. Repair of articular cartilage defects by tissue-engineered cartilage constructed with adipose-derived stem cells and acellular cartilaginous matrix in rabbits. Genet Mol Res 2014;13(2): 4599–606.

[39] Bauer C, Jeyakumar V, Niculescu-Morzsa E, Kern D, Nehrer S. Hyaluronan thiomer gel/matrix mediated healing of articular cartilage defects in New Zealand White rabbits-a pilot study. J Exp Orthop 2017;4(1):14.

[40] Orth P, Zurakowski D, Alini M, Cucchiarini M, Madry H. Reduction of sample size requirements by bilateral versus unilateral research designs in animal models for cartilage tissue engineering. Tissue Eng C Methods 2013;19(11):885–91.